Quaternary Research 71 (2009) 319–328

Contents lists available at ScienceDirect

Quaternary Research

journal homepage: www.elsevier.com/locate/yqres

Stable isotopes of a subfossil *Tamarix* tree from the Dead Sea region, Israel, and their implications for the Intermediate Bronze Age environmental crisis

Amos Frumkin *

Department of Geography, The Hebrew University of Jerusalem, 91905, Israel

ARTICLE INFO

Article history:
Received 19 December 2007
Available online 28 February 2009

Keywords:
Levant paleoclimate
Climate deterioration
Tree ring isotopes
Carbon isotopes
Nitrogen isotopes
Dead Sea level
Cave deposit
Radiocarbon
Salt karst
Sedom

ABSTRACT

Trees growing on the Mt. Sedom salt diapir, at the southern Dead Sea shore, were swept by runoff into salt caves and subsequently deposited therein, sheltered from surface weathering. A subfossil *Tamarix* tree trunk, found in a remote section of Sedom Cave is radiocarbon dated to between ~2265 and 1930 BCE. It was sampled in 109 points across the tree rings for carbon and nitrogen isotopes. The Sedom *Tamarix* demonstrates a few hundred years of ^{13}C and ^{15}N isotopic enrichment, culminating in extremely high $\delta^{13}C$ and $\delta^{15}N$ values. Calibration using modern *Tamarix* stable isotopes in various climatic settings in Israel shows direct relationship between isotopic enrichment and climate deterioration, particularly rainfall decrease. The subfossil *Tamarix* probably reflects an environmental crisis during the Intermediate Bronze Age, which subsequently killed the tree ~1930 BCE. This period coincides with the largest historic fall of the Dead Sea level, as well as the demise of the large regional urban center of the 3rd millennium BCE. The environmental crisis may thus explain the archaeological evidence of a shift from urban to pastoral culture during the Intermediate Bronze Age. This was apparently the most severe long-term historical drought that affected the region in the mid-late Holocene.

Introduction

The isotopic composition of vegetation can be used as a proxy for ancient air, water, and nutrients as well as environmental conditions (Epstein and Krishnamurthy, 1990; McCarroll and Loader, 2004). This paper attempts to reconstruct a climatic crisis during a crucial period of human history in the Levant, using variations in the natural abundance of carbon and nitrogen isotopes in stem cellulose of tree rings.

Where relative humidity or precipitation are the limiting factors to carbon isotope fractionation in trees, isotopic enrichment of ^{13}C in wood cellulose is an indicator of drought stress (Garten and Taylor, 1992; Stewart et al., 1995; Chen et al., 2000; Treydte et al., 2001; Warren et al., 2001; Leavitt et al., 2002; Swap et al., 2004; Gagen et al., 2004; McCarroll and Loader, 2004; Liu et al., 2004; Ferrio and Voltas, 2005; Leavitt, 2007). The reason is that under these conditions, relative humidity and soil moisture control stomatal conductance which in turn dominates the ratio of internal to external concentrations of CO_2 and the resultant C fractionation. In extremely arid regions such as Mt. Sedom, where the dominant stress factor influencing trees is a combination of high temperature and low precipitation, ^{13}C enrichment provides a strong indicator of such severe conditions (McCarroll and Loader, 2004).

In addition, studies from a variety of climatic regions and plant species reported significant negative correlation between annual rainfall and $\delta^{15}N$ values of wood cellulose in C3 plants (Heaton, 1987; Swap et al., 2004), although many other processes play a role too.

During early historic times, the impact of natural environmental deterioration on society could be significant, but is often debated due to the difficulty to differentiate between anthropogenic and natural effects. Four thousands years ago, anthropogenic impact on the environment was relatively small compared to the impact of natural environmental change on human society.

Mt. Sedom, at the south-western edge of the Dead Sea (Fig. 1A), is a unique site to study the pure environmental signal, and its effects on neighboring societies. The mountain itself has no archaeological remains, suggesting that human interventions, such as grazing, agriculture, pollution or habitation are negligible. Therefore, environmental conditions are believed to reflect mainly natural factors rather than human impact. In addition, other studied sites often have shallow groundwater reached by tree roots, precluding the determination of local $\delta^{13}C$ – climate relationship (Lipp et al., 1996). This limitation does not exist at Mt. Sedom, where no freshwater aquifer exists (Frumkin, 1994) and deep infiltration water become salinized, so the only water source is local rainfall and associated runoff.

In this study, a subfossil *Tamarix* tree trunk from Sedom Cave (Fig. 1B) is radiocarbon dated and isotopically analyzed in comparison with modern samples, in order to elucidate the nature of the Intermediate Bronze Age cultural crisis in the Dead Sea region. During this crisis the Early Bronze Age urban culture was abandoned and replaced by nomadic or semi-nomadic culture (e.g. Amiran, 1986; Dever, 1989; Finkelstein, 1989; Rast, 1987). The term

* Fax: +972 25820549.
E-mail address: msamos@mscc.huji.ac.il.

0033-5894/$ – see front matter © 2009 University of Washington. All rights reserved.
doi:10.1016/j.yqres.2009.01.009

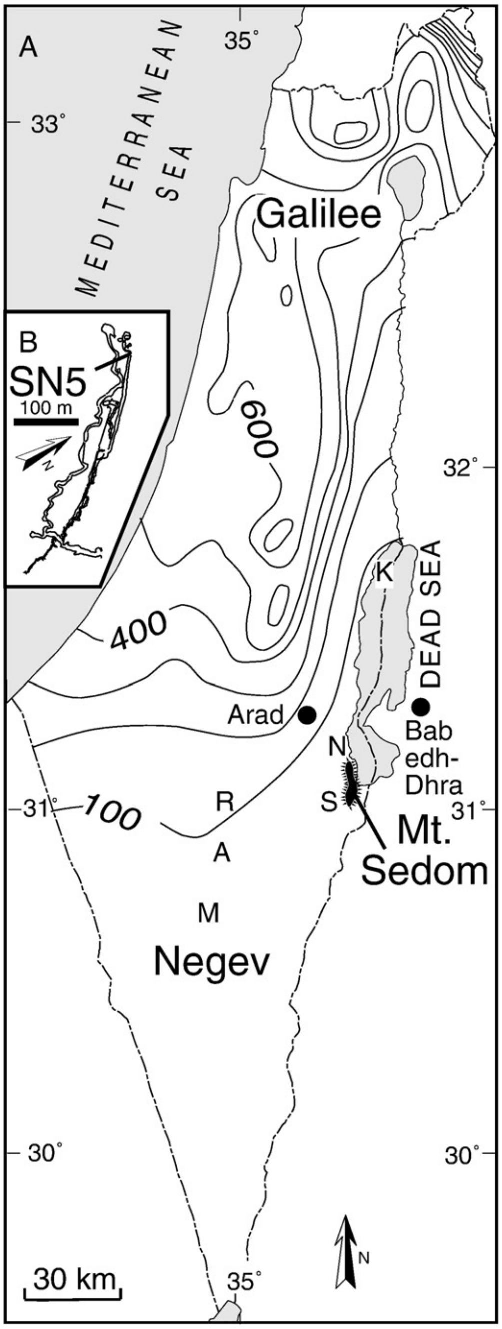

Figure 1. Map of the study area. (A) Rainfall map of Israel with site locations; lines are isohyets displaying modern mean annual precipitation (mm). The southern part of the Dead Sea, between Mt. Sedom and Bab edh-Dhra, dried up during the drought documented by the studied *Tamarix* SN5 tree trunk (Frumkin et al., 1991), and is also dry during recent decades. K = Kidron; N = Navit; R = Retamin; A = Avdat; M = Mizpeh Ramon; S = Sedom Cave. (B) Map of Sedom Cave in Mt. Sedom, with location of the studied SN5 *Tamarix* stem.

'Intermediate Bronze Age' for the period between ~2300 and 1900 BCE in the Levant is adopted here, because it has gained wide archaeological acceptance (Kenyon et al., 1974; Prag, 1974; Richard, 1980; Finkelstein, 1989; Stager, 1992).

Several researchers have attributed the Intermediate Bronze cultural crisis to a long-term severe drought (e.g. Bell, 1971; Crown, 1972; Richard, 1980; Rosen, 1989; Amiran, 1991; Nissenbaum, 1994). The climatic explanation of this event is not clear, and its possible relation with the NAO index is questionable, because the extent of NAO association with the present Middle East precipitation is debated (Cullen et al., 2000). Thus it remains important to study the exact nature of the Intermediate Bronze Age crisis. The subfossil *Tamarix* tree from Sedom Cave allows a new examination of this environmental crisis within the same region where settlements collapsed.

Regional setting and environmental record

The Dead Sea (Fig. 1A) is the terminal lake within the Dead Sea transform (Neev and Emery, 1967; Ben-Avraham and Lazar, 2006; Bookman et al., 2006). Its catchment covers ~43,000 km^2, extending over several climatic regions between moist Mediterranean climate in Lebanon and extremely arid Sinai Desert (Egypt). Present (CE 2007) lake level is 420 m below mean sea level, with a water depth of ~300 m. Its significant water sources are the Jordan River from the north and runoff/groundwater discharge along its east and west coasts, which mostly drain regions wetter than the Dead Sea itself (Greenbaum et al. 2006).

As a closed lake in an arid environment, the Dead Sea level is extremely sensitive to the climate of its catchment. This appealed to several generations of researchers (Bookman et al., 2006), of which the latest, based on comprehensive radiocarbon dating, are reviewed below.

Frumkin et al. (1991, 2001) presented a lake-level curve of the last 8000 yr, based on 33 radiocarbon dates of wood remains deposited in salt caves whose levels are controlled by the Dead Sea. Dating errors are ~100–200 yr depending on analytical errors and the residence time of dated material between its growth period and final deposition. Contamination is unlikely because the wood has been protected in a dry cave environment since deposition.

Kadan (1997) presented a lake-level record of the last 9000 yr, based on 20 radiocarbon dates of organic remains exposed along a new gully that was formed in the fast-retreating shores of the modern Dead Sea (Enzel et al. 2000). Based on similar deposits along the central Dead Sea, Bookman (Ken-Tor) et al. (2004) presented a lake-level curve of the last 4100 yr, with 46 radiocarbon ages of organic matter.

Migowski et al. (2006) analyzed sediment cores recovered from the Dead Sea, with 38 radiocarbon ages. Dating errors of Dead Sea organics may reach a few hundred yr, depending on their exposure to contamination from later Dead Sea waters and/or infiltrating meteoric water, in addition to the above-mentioned errors.

The various proxies agree that roughly around 2000 BCE, Dead Sea levels fell significantly by a few tens of meters (Kadan, 1997; Frumkin et al., 2001; Enzel et al., 2003; Bookman (Ken-Tor) et al., 2004). Consequently, the entire southern basin of the Dead Sea dried up (Neev and Emery, 1967) and sediments in the northern basin became more evaporitic (Migowski et al., 2006).

The above-mentioned proxies indicated a general environmental deterioration across the Dead Sea catchment around 2000 BCE. However, the resolution of the Dead Sea curve for this period is low, due to limitations of the proxies that have been previously used. In addition, it has not been possible to quantify and accurately date the Intermediate Bronze Age climatic crisis within the Dead Sea basin itself. This is the main purpose of the present paper.

Mt. Sedom is the exposed head of a salt diapir. Forming an elongated ridge 11 by 1.5 km, Mt. Sedom rises above the south-eastern shore of the Dead Sea (Zak, 1967), with an uplift rate of 6–9 mm/yr (Pe'eri et al., 2004; Weinberger et al., 2006).

Modern mean annual precipitation at Sedom (measured at the Sedom potash plant from 1960 to CE 2005) is 46 mm, ranging between 8 and 113 mm for individual years. The diapir consists mainly of rock-salt, piercing through tilted strata of younger lake evaporites and clastics, and covered by cap rock composed of anhydrite and clastics. The top of Mount Sedom is roughly tabular, with many small catchments up to 0.7 km^2 in area (Gerson, 1972; Frumkin, 1994). During infrequent rainstorms, runoff collects on the somewhat

https://doi.org/10.1016/j.yqres.2009.01.009 Published online by Cambridge University Press

Figure 2. *Tamarix jordanis* growing today on southern Mt. Sedom. Most of its parts have dried due to the present arid climate.

impervious cap rock and flows into fissures, creating salt caves. Nearly all caves have active stream passages as well as relict passages at higher levels. Over one hundred caves in Mt. Sedom provide a rich repository of Holocene subfossil wood. The wood originated from trees and shrubs which grew on Mt. Sedom, were swept by runoff into subterranean channels, and subsequently deposited therein. The channels were abandoned by the downcutting underground streams, and the wood was thereby sheltered from water and surface weathering agents.

Tamarix jordanis trees are on the verge of extinction today on Mt. Sedom, apparently due to the extremely arid climate (Fig. 2). This study sheds light on a previous extinction event of *Tamarix* on the mountain. *Tamarix* has been (and still is) common during the Holocene in most parts of Israel, including the vicinity of Mt. Sedom, where more water is available.

Methods

Radiocarbon dating was performed on three tree rings of the largest *Tamarix* tree stem (numbered SN5, Fig. 3). Two samples were dated at Geochron Laboratories, Cambridge, Massachusetts (Lab no. GX-31947 and GX-31948). Pretreatment: Each wood sample was carefully cut from a single tree ring. It was cleaned of dirt and split into small pieces. It was then treated with hot dilute HCl to remove any carbonates; with 0.1N dilute NaOH to remove humic acids and other organic contaminants; and a second time with dilute HCl. After washing and drying, the sample was combusted to recover carbon dioxide for the analysis by gas proportional counters. The conventional date calculation is based upon the Libby half-life (5570 yr) and includes a correction for fractionation, based on δ^{13}C values measurement. Calibration to calendar date was performed using OxCal program v. 3.10 (Bronk-Ramsey, 2001) based on the latest calibration curve (Reimer et al., 2004). The outermost ring of SN5 was dated earlier at the Weizmann Institute of Science (Lab no. 810D) (Frumkin et al., 1991). The results are compared with dates from the major Bronze Age settlement of the region (Fig. 4).

Stable C and N isotopes were measured in this study for whole-wood *Tamarix* samples, as suggested by McCarroll and Loader (2004), in order to estimate the average isotope signal for each sample. These include twelve modern samples (collected on CE 2005) from presently growing *Tamarix* stems representing the last decades on Mt. Sedom. Bulk samples of these twigs were analyzed for δ^{13}C and δ^{15}N values (Table 1). The modern δ^{13}C values were corrected in order to remove the effect of the decline of atmospheric δ^{13}C values due to fossil fuel combustion, by adding 1.6 and 1.4‰ for the Sedom samples (collected on CE 2005) and other arid regions (collected on CE 1992 by Lipp et al. (1996)) respectively, as suggested by McCarroll and Loader (2004). The corrections are based on interpolated data from the high precision records of δ^{13}C values in atmospheric CO_2 obtained from Antarctic ice cores (Francey et al., 1999). The modern samples are used to estimate the effect of precipitation on δ^{13}C values (Fig. 5).

Ten Holocene *Tamarix* cellulose of bulk samples from Mt. Sedom caves were analyzed for δ^{13}C values. Replicate analysis on standards and repeated measurement of a different part within the same twigs was performed on some samples (Table 2).

The secondary xylem of SN5 wood stem was sampled for stable isotopes with a knife blade and scalpel in 109 points across the tree rings (Table 3). The isotopic measurements were performed using the FlashEA 1112 nitrogen and carbon analyzer connected to Finnigan DELTAplusXL continuous flow mass spectrometer at the Institute of Earth Sciences, Hebrew University of Jerusalem. The precision of both δ^{13}C and δ^{15}N values is 0.15‰. Standards are PDB and N_2 for C and N isotopes respectively.

The above-mentioned data are compared with regional isotopic measurements performed previously on *Tamarix* wood samples from other regions in Israel. These were also corrected for industrial age atmospheric decline of δ^{13}C values.

Environmental control on the isotopic composition of trees in Mt. Sedom might involve multifactor complex processes. The less-significant factors are first identified below, in order to separate them from the dominant factors.

Subfossil wood is generally preserved in an excellent condition in Mt. Sedom Caves, due to the extremely dry, salty environment. It is very difficult to distinguish between a modern tree and a subfossil one (Fig. 3). It is assumed that under the sheltered cave site and extremely dry conditions, with no water reaching the subfossil wood, no diagenesis of the wood has taken place. Consequently, no significant remobilization of nitrogen isotopes between the tree rings is probable. If small-scale remobilization did occur, it might have influenced the details of the record rather than the entire isotopic range. The significant long-term variation of δ^{15}N values during the Intermediate Bronze Age (below), amounting to 21‰, is well beyond modern values, corroborating the above assumption.

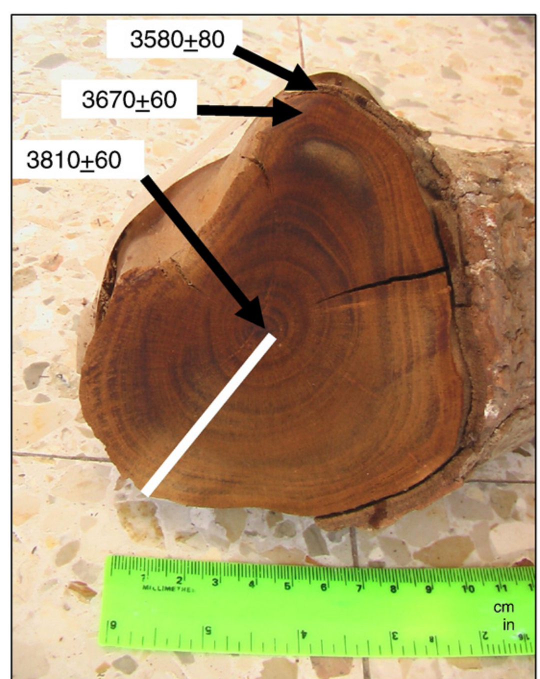

Figure 3. Cross section of SN5 *Tamarix* stem with conventional radiocarbon dates (see Fig. 4 for dating details and calibration). Samples for δ^{13}C and δ^{15}N values (Table 3, Fig. 6) were taken along the white line.

https://doi.org/10.1016/j.yqres.2009.01.009 Published online by Cambridge University Press

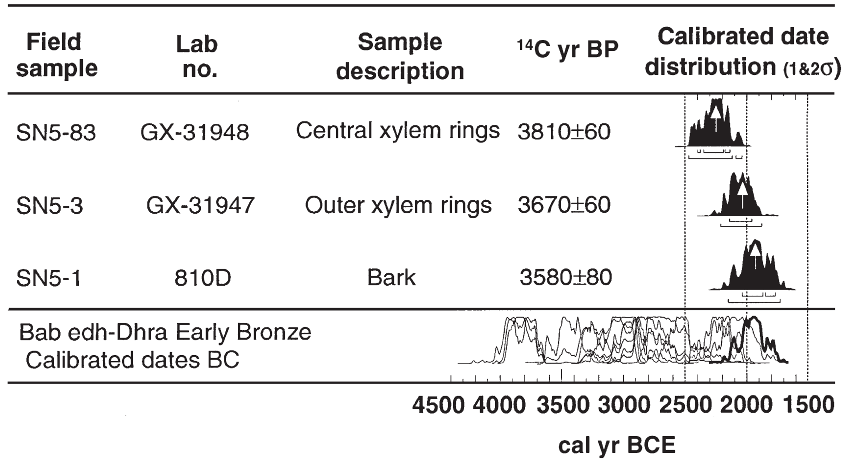

Figure 4. Radiocarbon dating of SN5 *Tamarix* stem cellulose. The conventional error quoted is $\pm 1\sigma$ as judged by the analytical data. The dating error distribution, as well as ± 1 and 2σ are presented. White arrows within the distribution curve indicate the peak probability of each calibrated radiocarbon date, used for age interpolation of the stable isotopes samples. A comparison with the range of calendar dates from the Early Bronze Age site of Bab edh-Dhra (Weinstein, 1984) demonstrates that the terminal phase of Bab edh-Dhra coincides with the life span of SN5, and the latest date of Bab edh-Dhra (bold line) is practically identical with the latest SN5 date.

Stable carbon isotope ratios of modern tree rings may be affected by variations in atmospheric CO_2. However, this is not the case for most of the Holocene, when variations in atmospheric CO_2 and $\delta^{13}C$ value of atmospheric CO_2 had little influence on the cellulose $\delta^{13}C$ values (Indermühle et al., 1999). Therefore no correction was applied for the effect of increasing atmospheric CO_2.

The $\delta^{13}C$ values of wood of different cambial age show no systematic differences after the juvenile period has been passed (Mayr et al., 2003). The isotopic trends demonstrated in SN5 continue well after its juvenile age, thus a 'juvenile effect' (McCarroll and Loader, 2004) cannot explain the observed variations.

Tamarix trees growing on top of Mt. Sedom cannot penetrate the cap rock which is ~50 m thick, so the underlying salt is unlikely stressing the trees directly.

Tamarix trees emit some salt to their environment, which may influence the immediate surroundings of the tree under normal conditions. However, on Mt. Sedom the soil and runoff water are relatively salty (Gerson, 1972; Frumkin, 1994) even without regard to *Tamarix* trees, so the additional salt emission may be neglected. Trees can grow in this arid environment where runoff is collected from local catchments into karst depressions. During high runoff events, water often accumulates in the depressions, followed by rapid infiltration that may flush the soil of its salts, depending on the water amount and salinity. During low precipitation events, only a shallow portion of the soil is wetted, followed by evaporation and increase of soil salinity. In Mt. Sedom, this process is dominant over soil salination by salt emission of the tree itself.

Table 1
Stable isotopes of modern *Tamarix* growing on the surface of Mt. Sedom (single analysis of each bulk sample)

Sample #	$\delta^{15}N$	$\delta^{13}C$	$\delta^{13}Cc$
m1	5.6	−22.7	−21.1
m2	5.7	−22.6	−21.0
m3	4.1	−22.2	−20.6
m4	5.7	−22	−20.4
m5	5.9	−22.6	−21.0
m6	9.1	−21.1	−19.5
m7	11.8	−22.6	−21.0
m8	9.9	−22.2	−20.6
m9	8.6	−21.3	−19.7
m10	10.2	−21.8	−20.2
m11	7.9	−21.6	−20.0
m12	10.6	−21.9	−20.3

$\delta^{13}Cc$ values are corrected for the industrial age atmospheric decline (see text).

Results

Modern twigs were collected (on CE 2005) from a living *Tamarix* shrub (Fig. 2) and their bulk wood was analyzed for C and N isotopes. Their $\delta^{13}C$ values range from −22.7 to −21.1‰, and their $\delta^{15}N$ values range from 4.1 to 11.8‰ (Table 1, Fig. 6A).

The main object of this study is the subfossil SN5 tree stem (Fig. 3), retrieved from a relict stream canyon at an upper level of Sedom Cave in southern Mt. Sedom (Fig. 1). SN5 must have grown within the Sedom Cave catchment on the mountain, and after dying it was carried by runoff water into the cave, where it got stuck between the walls of the narrowing (downward) canyon (Frumkin, 1998).

The growth period of SN5 is determined by three radiocarbon dates: 3810 ± 60 ^{14}C yr BP (GX-31948) for the central xylem rings, 3670 ± 60 ^{14}C yr BP (GX-31947) for the outer xylem rings, and 3580 ± 80 ^{14}C yr BP (810D) for the bark (Fig. 4). The peak probabilities of each calibrated radiocarbon date indicate that SN5 lived approximately from 2265 to 1930 BCE, roughly covering the Intermediate Bronze Age. SN5 remained stuck high and dry for ~3900 yr in the salty dry environment of the cave.

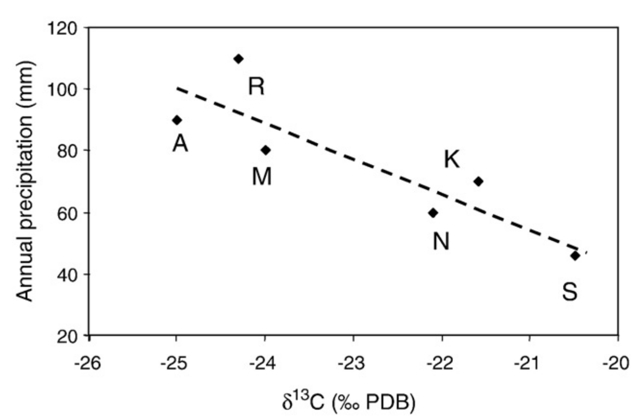

Figure 5. Modern mean annual precipitation vs. $\delta^{13}C$ values of modern *Tamarix jordanis* stem cellulose from arid sites in Israel in which the trees are not affected by shallow groundwater. Points K, N, R, A, and M represent individual modern samples of wholewood twigs for each site (see Fig. 1 for site location), after Lipp et al. (1996). Point S represents the average corrected value of twelve wholewood modern Sedom samples measured in this study ($\delta^{13}Cc$ values in Table 1). Precipitation is shown on the *Y* axis in order to extract precipitation values from $\delta^{13}C$ values of ancient wood. To facilitate this, a linear regression is used: Precipitation (mm) = −11.0 ($\delta^{13}C$) − 177 (R^2 = 0.76).

https://doi.org/10.1016/j.yqres.2009.01.009 Published online by Cambridge University Press

Table 2
Holocene Carbon isotopes of Mt. Sedom *Tamarix* twigs (bulk samples)

	Age		
Sample #	*cal yr CE/BCE*	*Age error*	*δ^{13}C*
MM1	130	120	−24.79
MM1*	130	120	−25.8
SN2	−2460	260	−22.06
SN2*	−2460	260	−21.3
MZ2	−3780	250	−20.61
MZ2*	−3780	250	−21.7
MZ3	−4020	30	−23.5
MZ5	−4840	110	−21.3

Calibrated radiocarbon dates after Frumkin et al. 1991.
* δ^{13}C measurement on another part of the same twig.

The significant narrowing (downward) of stream passages during the same period in many caves of Sedom is assigned to the Intermediate Bronze Age (Frumkin et al., 1991). The narrowing followed a well-dated stage of very wide stream passages ~3000 BCE. Downcutting of the canyons kept pace with the falling Dead Sea level, whose southern basin dried up during this period, indicating decreasing precipitation/evaporation ratio over the Dead Sea catchment.

The growth rings of SN5 can be distinguished due to the conspicuous zone of tangentially flattened fibers and wood parenchyma at the end of each growth ring. However, in the case of Mt. Sedom hyper-arid climate, consecutive years without significant rainfall are common (Gerson, 1972; Frumkin, 1994). Therefore, a growth ring does not necessarily represent a calendar year, particularly during droughts, so growth rings are not used here as cambial-age indicators.

The δ^{13}C values of SN5 rise throughout its growth history, with intermittent plateaus. The total lifetime increase is about 6‰, with fluctuations of 1 to 4‰. The total range of δ^{13}C values is from −25.7 up to −19.6‰. A few decades prior to its death, δ^{13}C values of SN5 climbed to the maximal (corrected) modern values, higher than all other Holocene Sedom values (Fig. 6). SN5 δ^{13}C values remained significantly high (maximum −19.7, mean −20.2‰) until the tree died.

SN5 demonstrates larger long-term increase of δ^{15}N values. These amount altogether to 21‰ rise, from −4.7‰ up to +16.3%.

Discussion

Modern δ^{13}C values

The δ^{13}C values of modern *Tamarix jordanis* stem cellulose in the arid parts of Israel have been shown to be climatically controlled (Lipp et al., 1996), ranging from −28.1‰ in the Galilee, under Mediterranean conditions (500 mm annual precipitation), to an average of −22‰ in the hyper-arid area of Mt. Sedom (present study). The measured modern δ^{13}C values range of *Tamarix* observed at Mt. Sedom (−22.7 to −21.1‰, Table 1), are significantly higher than in wetter regions. This strengthens the conclusion that climatic-environmental effects dominate over local effects such as soil salinity or competition (Lipp et al., 1996). The wide range of modern isotopic values in Sedom may be associated with the wide range of local annual precipitation (from 8 to 113 mm). The scatter of isotopic data points may also reflect variations associated with other environmental factors, such as temperature, relative humidity, soil salinity, or competition.

For calibrating the relation between modern δ^{13}C values of *Tamarix jordanis* and precipitation (Fig. 5), we use our corrected δ^{13}C data from presently growing *Tamarix* in Mt. Sedom (Table 1), and corrected modern tree values in various sites within the arid parts of Israel (Lipp et al., 1996). Figure 5 shows that in spite of the general scatter, a significant negative correlation between mean annual precipitation

Table 3
Stable isotopes of SN5 *Tamarix*, Mt. Sedom

Age, cal		
yr BCE	δ^{15}N	δ^{13}C
−2265	−4.11	−24.9
−2261.9	−4.73	−24.58
−2258.8	−3.92	−23.22
−2255.7	−2.39	−24.36
−2252.6	0.44	−23.5
−2249.5	1.63	−23.17
−2246.4	0.92	−23.55
−2243.3	2.87	−23.12
−2240.2	1.55	−24.2
−2237.1	2.57	−24.41
−2234	2.37	−25.56
−2230.9	3.48	−24.82
−2227.8	3.41	−24.68
−2224.7	4.7	−24.23
−2221.6	5.13	−24.41
−2218.5	5.43	−24.63
−2215.4	5.56	−24.38
−2212.3	5.3	−24.78
−2209.2	4.23	−24.49
−2206.1	4.4	−24.87
−2203	3.92	−25.58
−2199.9	5.84	−24.38
−2196.8	6.42	−23.62
−2193.7	5.68	−23.42
−2190.6	5.74	−23.59
−2187.5	5.46	−23.41
−2184.4	5.92	−22.6
−2181.2	5.24	−22.03
−2178.1	4	−21.5
−2175	4.5	−21.7
−2171.9	4.7	−21.6
−2168.8	5.7	−22
−2165.7	5	−21.7
−2162.6	5.4	−21.9
−2159.5	6.4	−22.4
−2156.4	6.3	−22.5
−2153.3	5.9	−22.5
−2150.2	5.5	−22.6
−2147.1	5.9	−22.9
−2144	6.2	−23.7
−2140.9	5.8	−23.2
−2137.8	5.6	−23.3
−2134.7	6.1	−25
−2131.6	6.1	−25.7
−2128.5	6.4	−25.3
−2125.4	6.5	−24.3
−2122.3	7.1	−24.5
−2119.2	7.4	−24.2
−2116.1	7.5	−23.9
−2113	7.3	−23.6
−2109.9	7	−23.7
−2106.8	6.8	−23.8
−2103.7	7.2	−23.7
−2100.6	7.2	−23.9
−2097.5	7.3	−23.4
−2094.4	7.2	−22.8
−2091.3	6.4	−23.4
−2088.2	7.7	−22.7
−2085.1	7.1	−23.2
−2082	7.8	−22.1
−2078.9	8.7	−22.2
−2075.8	6.4	−22.3
−2072.7	7.5	−22
−2069.6	7.5	−22
−2066.5	8.4	−21.6
−2063.4	8.4	−21.4
−2060.3	7.9	−21.1
−2057.2	8.4	−21.3
−2054.1	8.1	−21.2
−2051	8.3	−21.2
−2047.9	10.7	−21.6
−2044.8	8.5	−21.5
−2041.7	9.1	−22.3
−2038.6	9.8	−22.4

(continued on next page)

https://doi.org/10.1016/j.yqres.2009.01.009 Published online by Cambridge University Press

Table 3 (*continued*)

Age, cal yr BCE	$\delta^{15}N$	$\delta^{13}C$
−2035.5	9.9	−22.5
−2032.4	9.9	−22.7
−2029.3	9.9	−22.3
−2026.2	9.6	−21.8
−2023.1	10	−21.3
−2020	10.7	−19.9
−2016.9	11.3	−19.6
−2013.7	9.3	−20.6
−2010.6	10.1	−20.7
−2007.5	10	−21
−2004.4	10.3	−21.6
−2001.3	9.2	−21.3
−1998.2	10.1	−21.2
−1995.1	9.5	−21
−1992	9.8	−21.5
−1988.9	9.4	−20.8
−1985.8	9.4	−20.2
−1982.7	9.5	−19.8
−1979.6	9.4	−19.9
−1976.5	9.4	−19.9
−1973.4	9.7	−19.7
−1970.3	9.4	−19.7
−1967.2	9.5	−19.9
−1964.1	9.5	−19.7
−1961	10	−19.8
−1957.9	10.1	−19.9
−1954.8	8.9	−20.8
−1951.7	10.2	−20.7
−1948.6	10.9	−21.1
−1945.5	11.6	−19.9
−1942.4	11.1	−20.6
−1939.3	11.8	−20.5
−1936.2	13.3	−20.4
−1933.1	14.5	−20.3
−1930	16.3	−20.7

Calendar age is based on peak probabilities of three calibrated radiocarbon dates (white arrows in Fig. 4).

and corrected $\delta^{13}C$ values is observed, represented by the following linear regression:

$$\text{Precipitation (mm)} = -11.0\left(\delta^{13}C\right) - 177 \quad R^2 = 0.76 (p < 0.01). \quad (1)$$

The negative correlation with annual rainfall appears to be rather simplistic for a complex arid environment and the number of available measurements, but it is the most significant relationship between $\delta^{13}C$ values and any environmental parameter, including relative humidity (Lipp et al., 1996). It indicates the general negative correlation between precipitation and $\delta^{13}C$ values without a presumption of being an accurate relationship. The scatter about the line in Figure 5 suggests that other factors than rainfall also have an influence on $\delta^{13}C$. The minor wiggles of SN5 $\delta^{13}C$ (Fig. 6) may not represent real climatic change, although the major fluctuations (especially as they form a smooth trend) are probably meaningful (signifying wet/dry periods). Negative linear correlations between precipitation and $\delta^{13}C$ values for other tree species have been demonstrated in the past (e.g. Ferrio and Voltas, 2005).

In addition, a significant positive correlation exists between (frequency and magnitude of) large runoff events and annual precipitation in Mt. Sedom and other arid areas of Israel (Gerson, 1972; Kahana et al., 2002; Greenbaum et al., 2006). Assuming that the general setting at Mt. Sedom has not changed considerably during the Holocene, the current relation between corrected $\delta^{13}C$ values and precipitation may be used to estimate rainfall in the past.

The paleo-$\delta^{13}C$ record

Tamarix wood remains from Mt. Sedom whose calibrated radiocarbon dates fall between 4840 BCE and CE 130 (Frumkin et al., 1991) show $\delta^{13}C$ values ranging from −25.8 to −20.6‰ (Table 2). These values are similar and mostly lower than corrected modern values (Fig. 6A; Table 1) suggesting that during the Holocene, *Tamarix* trees could thrive abundantly enough to be eventually swept into caves, mostly when climate was wetter than today.

As explained above, the isotopic enrichment of ^{13}C with time in SN5 is likely linked to deteriorating moisture conditions that reduce stomatal conductance and hence the concentration ratio of leaf intercellular CO_2 to air CO_2, thus resulting in ^{13}C enrichment.

Assuming that Eq. (1), the apparent empirical relation between modern precipitation and $\delta^{13}C$ values, has been valid through the mid-late Holocene, a quantitative evaluation of past precipitation is attempted (Fig. 7). A general drying pattern is inferred, with large fluctuations. An intense drying event occurred ~2020 BCE, but its short duration allowed the tree to survive, probably by using residual soil moisture. Finally, around 1980 BCE, a prolonged multi-year drought started, which apparently caused the death of the tree, ~1930 BCE. The precipitation during the final period apparently dropped below the present level, albeit not significantly. This is in agreement with the almost total absence of *Tamarix* trees in Mt. Sedom today, and the poor condition of what remains (Fig. 2).

The paleo-$\delta^{15}N$ record

Further insight into the Intermediate Bronze Age climate may be obtained by the wood $\delta^{15}N$ values. Modern $\delta^{15}N$ values of *Tamarix* wood at Mt. Sedom range from 4.1 to 11.8‰ (Table 1, Fig. 6A), reflecting the present hyper-arid environment of the region. Isotopic discrimination of nitrogen is indicative of N cycling, and closely associated with precipitation, although the various processes are not well understood (above). Enrichment of ^{15}N associated with drier conditions has been demonstrated for plants in several arid regions. The large temporal enrichment (21‰) observed in SN5 indicates various biogeophysical processing and cycling of N, most probably associated with decreased rainfall, with more open N cycling and smaller losses relative to moister conditions (Swap et al., 2004). As SN5 obviously grew in the same site all its life, the climatic effects seem to be more significant than other environmental effects, whose role is beyond the scope of this study.

The growth period of SN5 can be subdivided into three parts (Figs. 6, 8): The initial steep rising of $\delta^{15}N$ values (Fig. 6B) may reflect drying and/or competition with other plants growing in the same niche during SN5 juvenile period. Following these first years, however, the continuous enrichment of ^{15}N values, which generally correlates with ^{13}C enrichment (Fig. 8), most likely reflects environmental deterioration. During the major part of SN5's life span, $\delta^{15}N$ values were within the modern range. Present day correlation between $\delta^{15}N$ values and rainfall for various plant species and ecological settings (Heaton, 1987; Swap et al., 2004) corroborates the conclusion that climate became increasingly drier during the life span of SN5, starting as wetter than today and becoming drier than today when the tree died.

An abrupt unprecedented jump of 4.5‰ in the SN5 $\delta^{15}N$ record (arrow in Fig. 6B) occurred just before the tree died. In addition to the prolonged gradual drying, as indicated by the rising isotopic values, the *coup de grace* must have been given by a severe extended drought, as indicated also by the $\delta^{13}C$ record (above). At the end of this drought, $\delta^{15}N$ values rose for the first time above the modern range, indicating severe environmental stress on the tree, which was probably initiated by lower rainfall, and accompanied by evaporation and salination of the unflushed soil. SN5 did not survive this final event. The $\delta^{13}C$ – $\delta^{15}N$ relation during this last period (Fig. 8) shifts to a new mode, probably associated with the extreme stress.

https://doi.org/10.1016/j.yqres.2009.01.009 Published online by Cambridge University Press

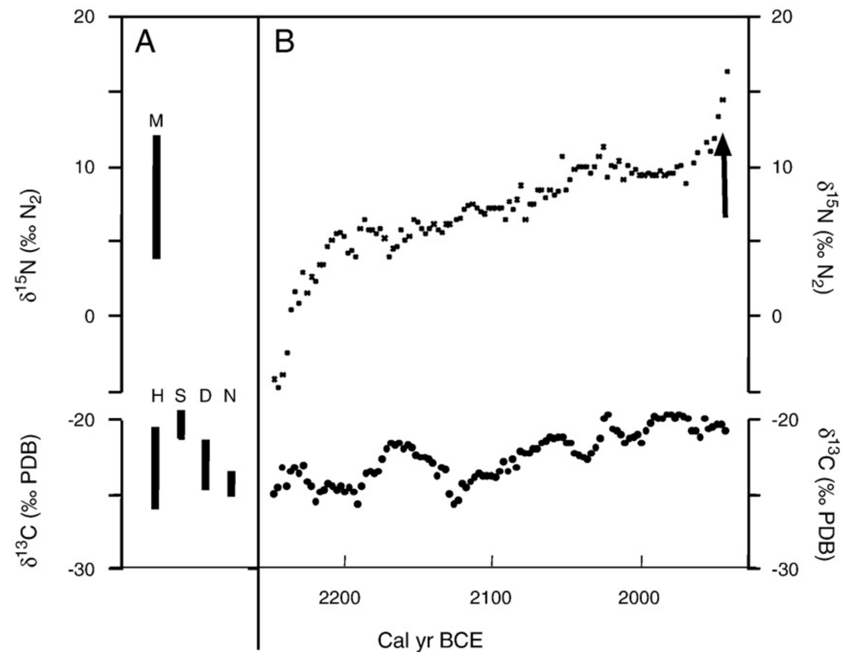

Figure 6. Compilation of $\delta^{13}C$ and $\delta^{15}N$ values of wood cellulose of *Tamarix* samples from Israel. Isotopic measurement errors are within the size of the data points/lines. (A) Modern and Holocene ranges of isotopic values (no horizontal scale): M — modern $\delta^{15}N$ range at Mt. Sedom ($n=12$ samples); H — Holocene $\delta^{13}C$ range, Mt. Sedom caves subfossil wood ($n=10$). Note that the maximal Holocene $\delta^{13}C$ value is close to the SN5 high range, suggesting additional dry periods; S — modern $\delta^{13}C$ range at Mt. Sedom ($n=12$ samples); D — modern $\delta^{13}C$ range, other sites in the Dead Sea region ($n=11$) (Lipp et al., 1996; Yakir et al., 1994); N — modern $\delta^{13}C$ range, Negev ($n=5$) (Lipp et al., 1996). Modern $\delta^{13}C$ values (S,D,N) are corrected for industrial age atmospheric depletion (see text). (B) Isotopic composition of SN5 from Mt. Sedom, with chronology based on the peak probability of each calibrated radiocarbon date (white arrows in Fig. 4). Black arrow indicates the terminal abrupt rise of $\delta^{15}N$ values.

Environmental change

In the arid environment of the Dead Sea, vegetation proves to be very sensitive to precipitation changes. Subfossil oaks (*Quercus calliprinos* Webb.) from three of the widest Mt. Sedom cave passages indicate that the highest precipitation occurred ~3000 BCE (Frumkin et al., 1991). This was followed by gradual drying during the 3rd millennium BCE, culminating with extreme climatic crisis evidenced by the stable isotopes of SN5. This crisis must have affected both vegetation and human populations of the region.

An experimental desert farm in the Negev showed that the number of successive drought years is the limiting factor for the life span of trees (Evenari et al., 1971). Defining a drought year as one with $<0.8\sigma$ of the modern long-term average annual rainfall (Enzel et al., 2003), no more than three successive drought years have been recorded at Sedom between CE 1960 and 2005. This allows some perennial vegetation, such as *Tamarix*, to survive today on Mt. Sedom, using residual soil moisture from the previous concentrated runoff event. This situation is reflected in the modern $\delta^{13}C$ and $\delta^{15}N$ values. It can be inferred that drier conditions would deplete the soil moisture, lead to higher isotopic values, and ultimately to the death of the surviving trees.

If the modern correlation between precipitation and $\delta^{13}C$ values (Eq. (1)) is used to infer past precipitation, than the following conclusion may be reached: Since ~1980 BCE until the death of SN5, mean annual rainfall fell from ~twice the modern average to

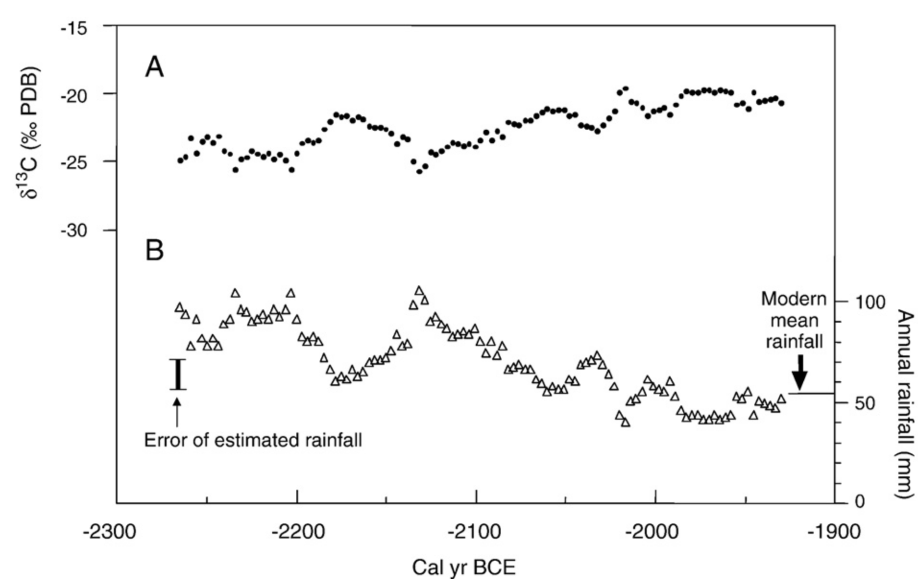

Figure 7. (A) $\delta^{13}C$ record of the subfossil SN5 *Tamarix* tree stem. (B) Calculated paleo-rainfall using the $\delta^{13}C$ record and the modern calibration (using Eq. (1), Fig. 5, and its error).

https://doi.org/10.1016/j.yqres.2009.01.009 Published online by Cambridge University Press

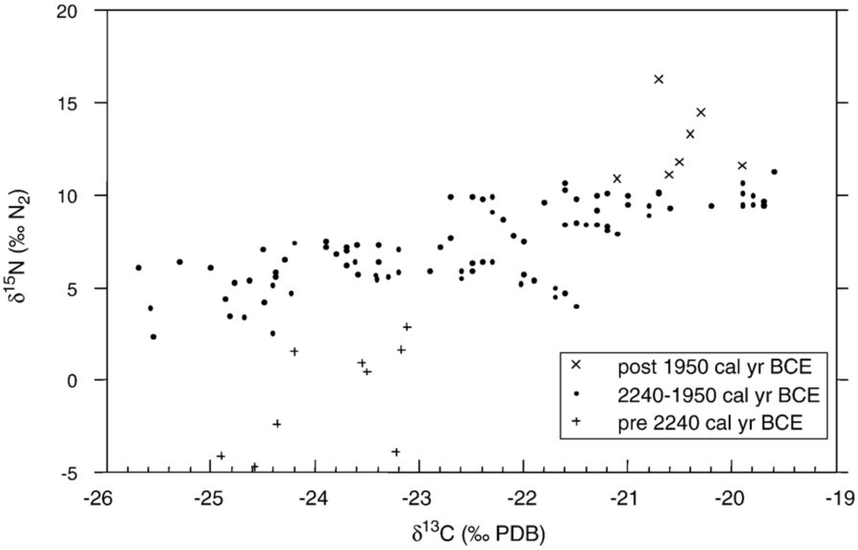

Figure 8. The $\delta^{13}C$ – $\delta^{15}N$ relationship in SN5. Three groups of points are observed: (1) Young age, before 2240 cal yr BCE; (2) The main growth period, from 2240 to 1950 cal yr BCE; (3) Terminal growth, after 1950 cal yr BCE. The three groups demonstrate different $\delta^{13}C$ – $\delta^{15}N$ correlations (see text).

~modern average of Mt. Sedom (Fig. 7). The conservative age model suggests that this dry event persisted for more than 50 yr, subsequently depleting soil moisture and eliminating perennial vegetation. A more realistic age model would consider the slower growth of tree rings during dryer years, thus the dry period must have persisted for longer time. If an extremely dry year brings about a natural drop of 40–50 cm yr^{-1} of Dead Sea level (Enzel et al., 2003), than the >45 m drop of Dead Sea level between 2200 and 1900 BCE (Frumkin et al., 1991; Bookman (Ken-Tor) et al., 2004; Migowski et al., 2006) could have actually occurred during a prolonged drought of at least 100 yr. This corroborates the possibility that the multi-year drought that started ~1980 BCE continued after the death of SN5, at least until ~1880 BCE. This is in agreement with a large drop of the Dead Sea level.

The inferred prolonged drought must have affected also the discharge of perennial springs and streams of the region, including those recharged by rainfall over the surrounding mountains. The impact on human society is discussed below.

Possible impact on human society

Several Bronze Age archaeological sites are known along the south-eastern part of the Dead Sea (Rast, 1987). The largest site, Bab edh-Dhra, has been intensively excavated; the wide range of archaeological finds and radiocarbon dates indicate that it was inhabited during the third millennium BCE (Rast, 1987; Weinstein, 1984). Its late radiocarbon dates correspond well with the dates of SN5. These last dates of Bab edh-Dhra reflect the culmination of a successful urban stage in the entire region. It is interesting to note that the final dates of the SN5 tree and Bab edh-Dhra (Weinstein, 1984) are very similar, 3580 ± 80 ^{14}C yr BP (810D) and 3590 ± 70 ^{14}C yr BP (SI-2875) respectively (for cal age distribution see Fig. 4, bottom right). These results suggest a possible synchronous impact of the environmental crisis on both flora and human habitation in the southern Dead Sea region. The perennial stream running below Bab edh-Dhra could support some human activity during the Intermediate Bronze Age, until the final severe prolonged drought. West of the Dead Sea, however, the urban center of Arad was deserted earlier, probably because it relied entirely on local water supply, without any perennial stream (Weinstein, 1984; Amiran, 1986; Yair and Garti, 1996).

The impact of multi-year droughts could thus be more severe than just decreasing mean annual precipitation. A desert settlement could survive short droughts by storing food or capital from wetter years, for consumption in years of drought. However, water storage techniques were hardly developed yet. Consequently, the urban-sedentary society was not able to withstand the effects of a prolonged drought as soon as water was unavailable within the settlements, agricultural deteriorated, and food reserves were exhausted. A major earthquake could also contribute to the severe situation and the inability to survive this harsh period.

The documented history of the Intermediate Bronze Age in the Dead Sea region is vague, due to the lack of contemporary writings from this area. The biblical accounts in the book of Genesis are of special interest, although they can hardly be tested scientifically, due to their ephemeral nature, remote period, or vague geographic setting. However, the pastoral environment of the patriarchs period (Gen. 12–47) stand out in its reasonably well known setting. These chapters also record an echo of recurrent drought and famine periods (Gen. 12:10, 26:1, 42:5, 47:4–13), which forced the nomads to find refuge in Egypt. The scientific approaches towards these accounts vary, but scholars who adopt their historic background commonly relate them to the socioeconomic situation of pastoral nomads in the Near East during the late third and the early second millennium BCE (e.g. Glueck, 1959; Albright, 1963; Speiser, 1964; Grintz, 1983; Rast, 1987; Nissenbaum, 1994; Issar and Zohar, 2004; Meitlis, 2006). The findings of the present study may further attest to the authentic background of these early traditions.

Conclusion

Carbon and nitrogen isotopes of stem wood in arid regions are found to be highly sensitive to environmental change. Isotopic enrichment of ^{13}C in wood cellulose is known to be related to environmental stress under dry conditions. A negative correlation is indeed observed in Israel between modern precipitation and $\delta^{13}C$ values of *Tamarix* tree rings. This correlation is used for analyzing a subfossil *Tamarix* stem showing that rainfall decreased substantially through the Intermediate Bronze Age in the Dead Sea region. This find is backed by the enrichment of ^{15}N in the *Tamarix* tree rings, which also seems to be dominated by precipitation in the extremely arid climate of Mt. Sedom.

The documented drying period culminated with the death of the *Tamarix* tree around 1930 BCE, caused by a prolonged severe drought lasting >100 yr. Although mean annual rainfall during this severe drought was not considerably lower than today, it probably comprised many consecutive years with almost no rainfall. The severe drop of Dead Sea level during the Intermediate Bronze Age amounted to

https://doi.org/10.1016/j.yqres.2009.01.009 Published online by Cambridge University Press

~45 m, which can be compared with the last century's drop (albeit anthropogenic) of Dead Sea level.

The environmental deterioration evidenced in the subfossil wood could be the natural background and driving force behind the human transitions of the Intermediate Bronze Age. Regional archaeology suggests that the impact on human population was the gradual abandonment of the 3rd millennium BCE urban centers, and a shift to a pastoral-rural society. The new economy, based primarily on animal husbandry, took advantage of a higher degree of mobility and could adjust itself to the decreasing seasonal availability of pasture and water during the environmental crisis.

A historic echo of this situation may be found in the patriarchs stories of Genesis. This present study contributes to the debate concerning the cause and effect of cultural changes in human history, which gained some basic ideas from the Levant (e.g. Dever, 1989; deMenocal, 2001; Weiss and Bradley, 2001; Issar and Zohar, 2004).

Acknowledgments

I thank N. Liphschitz of the Tel Aviv University and E. Werker of the Hebrew University of Jerusalem for identifying the subfossil wood samples, E. Raz of the Dead Sea Research and Development, Y. Elitzur of Michlelet Hertzog, J. Charrach of the Dead Sea works, U. Dayan and Y. Barkan of the Hebrew University of Jerusalem, S. Lev-Yadun of the Haifa University, and H. Bruins of the Ben Gurion University of the Negev for their help and advice; the team of the Cave Research Section, The Hebrew University of Jerusalem, for fieldwork assistance. This study was supported by grants from the Dead Sea Research and Development and the Science Ministry of Israel.

References

Albright, W.F., 1963. The Biblical Period from Abraham to Ezra. Harper & Row, New York, p. 118.

Amiran, R., 1986. The fall of the Early Bronze age II city of Arad. Israel Exploration Journal 36, 74–76.

Amiran, D.H.K., 1991. The climate of the ancient Near East. The early third millennium in the northern Negev of Israel. Erdkunde 45 (3), 153–162.

Bell, A., 1971. The Dark Ages in Ancient History. I. The first Dark Age in Egypt. American Journal of Archaeology 75, 1–26.

Ben-Avraham, Z. and Lazar, M., 2006. The structure and development the Dead Sea Basin: Recent studies. In: Y. Enzel, A. Agnon and M. Stein (Editors), New frontiers in Dead Sea paleoenvironmental research. GSA Special Paper 401, Boulder, pp. 1–13.

Bookman (Ken-Tor), R., Enzel, Y., Agnon, A., Stein, M., 2004. Late Holocene lake levels of the Dead Sea. GSA Bulletin 116 (5/6), 555–571.

Bookman, R., Bartov, Y., Enzel, Y. and Stein, M., 2006. Quaternary lake levels in the Dead Sea Basin: Two centuries of research. In: Y. Enzel, A. Agnon and M. Stein (Editors), New frontiers in Dead Sea paleoenvironmental research. GSA Special Paper 401, Boulder, pp. 155–170.

Bronk-Ramsey, C., 2001. Development of the radiocarbon program OxCal. Radiocarbon 43 (2A), 355–363.

Chen, T., et al., 2000. Study on the climatic significance of fir tree ring $\delta^{13}C$ from Zhaosu County, Xinjiang, China. Journal of Glaciology and Geocryology 22 (4), 347–351.

Crown, A.D., 1972. Toward a reconstruction of the climate of Palestine 8000 BC — 0 BC. Journal of Near Eastern Studies 31, 312–330.

Cullen, H.M., deMenocal, P.B., Hemming, S., Hemming, G., Brown, F.H., Guilderson, T., Sirocko, F., 2000. Climate change and the collapse of the Akkadian empire: evidence from the deep sea. Geology 28 (4), 379–382.

deMenocal, P.B., 2001. Cultural responses to climate change during the late Holocene. Science 292 (5517), 667.

Dever, W.G., 1989. The collapse of the urban Early Bronze age in Palestine: toward a systematic analysis. In: de Miroschedji, P. (Ed.), L'urbanisation de la Palestine à l'âge du Bronze Ancien. BAR International Series, Oxford, pp. 225–246.

Enzel, Y., Kadan, G., Eyal, Y., 2000. Holocene earthquakes inferred from a fan-delta sequence in the Dead Sea graben. Quaternary Research 53, 34–48.

Enzel, Y., Bookman (Ken-Tor), R., Sharon, D., Gvirtzman, H., Dayan, U., Ziv, B., Stein, M., 2003. Late Holocene climates of the Near East deduced from Dead Sea level variations and modern regional winter rainfall. Quaternary Research 60, 263–273.

Epstein, S., Krishnamurthy, R.V., 1990. Environmental information in trees. Philosophical Transactions of the Royal Society of London A 330, 427–439.

Evenari, M., Shanan, L., Tadmor, N.H., 1971. The Negev — The Challenge of a Desert. Harvard University Press, Cambridge, Mass.

Ferrio, J.P., Voltas, J., 2005. Carbon and oxygen isotope ratios in wood constituents of *Pinus halepensis* as indicators of precipitation, temperature and vapour pressure deficit. Tellus Series B – Chemical and Physical Meteorology 57B, 164–173.

Finkelstein, I., 1989. Further observations on the socio-demographic structure of the Intermediate Bronze Age. Levant 21, 129–140.

Francey, R.J., Allison, C.E., Etheridge, D.M., Trudinger, C.M., Enting, I.G., Leuenberger, M., Langenfelds, R.L., Michel, E., Steele, L.P., 1999. A 1000-year high precision record of $\delta^{13}C$ in atmospheric CO_2. Tellus 51B, 170–193.

Frumkin, A., 1994. Hydrology and denudation rates of halite karst. Journal of Hydrology 162, 171–189.

Frumkin, A., 1998. Salt cave cross sections and their paleoenvironmental implications. Geomorphology 23, 183–191.

Frumkin, A., Carmi, I., Zak, I. and Magaritz, M., 1991. The Holocene climatic record of the salt caves of Mount Sedom, Israel: The Holocene, 1,3, 191–200.

Frumkin, A., Kadan, G., Enzel, Y., Eyal, Y., 2001. Radiocarbon chronology of the Holocene Dead Sea: attempting a regional correlation. Radiocarbon 43, 2C, 1179–1190.

Gagen, M., McCarroll, D., and Edouard, J.L., 2004. Latewood width, maximum density, and stable carbon isotope ratios of pine as climate indicators in a dry subalpine environment, French Alps. Arctic, Antarctic and Alpine Research, 36, 2, 166–171.

Garten, C.T., Taylor, G.E., 1992. Foliar $\delta^{13}C$ within a temperate deciduous forest: spatial, temporal and species sources of variation. Oecologia 90, 1–7.

Gerson, R., 1972. Geomorphic processes of Mount Sdom. PhD thesis (in Hebrew, English abstract), The Hebrew University, Jerusalem.

Glueck, N., 1959. Rivers in the Desert. New York.

Greenbaum, N., Ben-Zvi, A., Haviv, I. and Enzel, Y., 2006. The hydrology and paleohydrology of the Dead Sea tributaries. In: Y. Enzel, A. Agnon and M. Stein (Editors), New frontiers in Dead Sea paleoenvironmental research. GSA Special Paper 401, Boulder, pp. 63–93.

Grintz, Y.M., 1983. The Book of Genesis, its Uniqueness and Antiquity (Hebrew). Magnes, Jerusalem.

Heaton, T.H.E., 1987. $^{15}N/^{14}N$ ratios of plants in South Africa and Namibia: relationship to climate and coastal/saline environment. Oecologia 74, 236–246.

Indermühle, T.E., Stocker, T.F., Joos, F., Fischer, H., Smith, H.J., Wahlen, M., Deck, B., Mastroiann, D., Tchhumi, J., Blunier, T., Meyer, R., Stauffer, B., 1999. Holocene carbon-cycle dynamics based on CO_2 trapped in ice at Taylor Dome, Antarctica. Nature 398, 121–126.

Issar, A.S., Zohar, M., 2004. Climate Change – Environment and Civilization in the Middle East. Springer – Heidelberg, Berlin – New York.

Kadan, G., 1997. Evidence of Dead-Sea level fluctuations and neotectonic events in the Holocene fan-delta of Nahal Darga. M.Sc. Thesis (in Hebrew, English abstract), Ben Gurion University of the Negev, Be'er Sheba, 54 pp.

Kahana, R., Ziv, B., Enzel, Y., Dayan, U., 2002. Synoptic climatology of major floods in the Negev Desert, Israel. International Journal of Climatology 22, 867–882.

Kenyon, K.M., Bottero, J. and Posener, G., 1974. Syria and Palestine c. 2160–1780 B.C., Cambridge Ancient History, 3rd revised ed., vol. I (2). Cambridge University, Cambridge, pp. 532–594.

Leavitt, S.W., 2007 Regional expression of the 1988 U.S. Midwest drought in seasonal delta C-13 of tree rings Journal-of-Geophysical-Research, D:-Atmospheres, 112 (D6), Art. No. D06107

Leavitt, S.W., Wright, W.E., Long, A., 2002. Spatial expression of ENSO, drought, and summer monsoon in seasonal $\delta^{13}C$ of ponderosa pine tree rings in southern Arizona and New Mexico. Journal-of-Geophysical-Research, D:-Atmospheres 107 (18) 3-1-3-10.

Lipp, J., Trimborn, P., Edwards, T., Waisel, Y., Yakir, D., 1996. Climatic effects on the $\delta^{18}O$ and $\delta^{13}C$ of cellulose in the desert tree *Tamarix jordanis*. Geochim. Cosmochim. Acta 60 (17), 3305–3309.

Liu, Y., Ma, L., Leavitt, S.-W., Cai, Q., Liu, W., 2004. A preliminary seasonal precipitation reconstruction from tree-ring stable carbon isotopes at Mt. Helan, China, since AD 1804. Global and Planetary Change 41 (3–4), 229–239.

Mayr, C., Frenzel, B., Friedrich, M., Spurk, M., Stichler, W., Trimborn, P., 2003. Stable carbon- and hydrogen-isotope ratios of subfossil oaks in southern Germany: methodology and application to a composite record for the Holocene. The Holocene 13 (3), 393–402.

McCarroll, D., Loader, N.J., 2004. Stable isotopes in tree rings. Quaternary Science Reviews 23, 771–801.

Meitlis, Y., 2006. Digging the Bible (in Hebrew). Rubin Mass, Jerusalem, 287 pp.

Migowski, C., Stein, M., Prasad, S., Negendank, J.F.W., Agnon, A., 2006. Holocene climate variability and cultural evolution in the Near East from the Dead Sea sedimentary record. Quaternary Research 66, 421–431.

Neev, D., Emery, K.O., 1967. The Dead Sea, depositional processes and environments of evaporites. Geological Survey of Israel Bulletin 41, 1–147.

Nissenbaum, A., 1994. Sodom, Gomorrah and the other lost cities of the plain — a climatic perspective. Climatic Change 26 (4), 435–446.

Pe'eri, S., Zebker, H.A., Ben-Avraham, Z., Frumkin, A., Hall, J.K., 2004. Spatially-resolved uplift rate of the Mount Sedom (Dead Sea) salt diapir from InSAR observations. Israel Journal of Earth Sciences 2 (2), 99–106.

Prag, K., 1974. The Intermediate Early Bronze-Middle Bronze Age: an interpretation of the evidence from Transjordan, Syria and Lebanon. Levant 6, 69–116.

Rast, W.E., 1987. Bab edh-Dhr'a and the origin of the Sodom saga. In: Perdue, L.G., Toombs, L.E., Johnson, G.L. (Eds.), Archaeology and Biblical Interpretation. John Knox Press, Atlanta, pp. 185–201.

Reimer, P.J., Baillie, M.G.L., Bard, E., Bayliss, A., Beck, J.W., Bertrand, C., Blackwell, P.G., Buck, C.E., Burr, G., Cutler, K.B., Damon, P.E., Edwards, R.L., Fairbanks, R.G., Friedrich, M., Guilderson, T.P., Hughen, K.A., Kromer, B., McCormac, F.G., Manning, S., Bronk Ramsey, C., Reimer, R.W., Remmele, S., Southon, J.R., Stuiver, M., Talamo, S., Taylor, F.W., J., v.d.P., Weyhenmeyer, C.E., 2004. IntCal04: calibration issue. Radiocarbon 46 (3), 1029–1058.

Richard, S., 1980. Toward a consensus of opinion on the end of the Early Bronze age in Palestine-Transjordan. Bulletin of the American Schools of Oriental Research 237, 5–34.

https://doi.org/10.1016/j.yqres.2009.01.009 Published online by Cambridge University Press

Rosen, A.M., 1989. Environmental change at the end of Early Bronze age Palestine. In: de Miroschedji, P. (Ed.), L'urbanisation de la Palestine à l'âge du Bronze Ancien. BAR International Series, Oxford, pp. 247–255.
Speiser, E.A., 1964. The Anchor Bible — Genesis. Doubleday, New York, p. 377.
Stager, L.E., 1992. The periodization of Palestine from Neolithic through Early Bronze times. In: Ehrlich, R.W. (Ed.), Chronologies in Old World Archaeology (third edition). Chicago: The University of Chicago Press, Chicago, pp. 22–41.
Stewart, G.R., Turnbull, M.H., Schmidt, S., 1995. ^{13}C Natural abundance in plant communities along a rainfall gradient: a biological intergrator of water availability. Australian Journal of Plant Physiology 22, 51–55.
Swap, R.J., Aranibar, J.N., Dowty, P.R., Gilhooly III, W.P., Macko, S.A., 2004. Natural abundance of ^{13}C and ^{15}N in C3 and C4 vegetation of southern Africa: patterns and implications. Global Change Biology 10, 350–358.
Treydte, K., Schleser, G.H., Schweingruber, F.H., Winiger, M., 2001. The climatic significance of $\delta^{13}C$ in subalpine spruces (Lotschental, Swiss Alps). Tellus-Series-B:-Chemical-and-Physical-Meteorology 53 (5), 593–611.
Warren, C.R., McGrath, J.F., Adams, M.A., 2001. Water availability and carbon isotope discrimination in conifers. Oecologia 127, 476–486.
Weinberger, R., Begin, Z.B., Waldmann, N., Gardosh, M., Baer, G., Frumkin, A. and Wdowinski, S., 2006. Quaternary rise of the Sedom Diapir, Dead Sea basin. In: Y. Enzel, A. Agnon and M. Stein (Editors), New frontiers in Dead Sea paleoenvironmental research, GSA Special Paper 401. GSA, Boulder, pp. 33–51.
Weinstein, J.M., 1984. Radiocarbon dating in the Southern Levant. Radiocarbon 26 (3), 297–366.
Weiss, H., Bradley, R.S., 2001. What drives social collapse? Science 291, 609–610.
Yair, A., Garti, A., 1996. The water supply at ancient Arad. In: Amiran, R., Ilan, O. (Eds.), Early Arad. The Israel Museum and the Israel Exploration Society, Jerusalem, pp. 127–138.
Yakir, D., Gat, J., Issar, A., Adar, E., Trimbom, P., Lipp, J., 1994. ^{13}C and ^{18}O of wood from the Roman siege rampart in Masada (AD 70–73): evidence for a less arid climate for the region. Geochim. Cosmochim. Acta 58 (16), 3535–3539.
Zak, I., 1967. The geology of Mount Sedom. PhD thesis (in Hebrew, English abstract), The Hebrew University, Jerusalem, 208 pp.